Classical and Slow-Binding Inhibitors of Human Type II Arginase†

Diana M. Colleluori and David E. Ash*

Department of Biochemistry, Temple University School of Medicine, 3420 North Broad Street, Philadelphia, Pennsylvania 19140

Received April 17, 2001; Revised Manuscript Received June 4, 2001

ABSTRACT: Arginases catalyze the hydrolysis of L-arginine to yield L-ornithine and urea. Recent studies indicate that arginases, both the type I and type II isozymes, participate in the regulation of nitric oxide production by modulating the availability of arginine for nitric oxide synthase. Due to the reciprocal regulation between arginase and nitric oxide synthase, arginase inhibitors have therapeutic potential in treating nitric oxide-dependent smooth muscle disorders, such as erectile dysfunction. We demonstrate the competitive inhibition of the mitochondrial human type II arginase by N^{ω}-hydroxy-L-arginine, the intermediate in the reaction catalyzed by nitric oxide synthase, and its analogue N^{ω}-hydroxy-*nor*-L-arginine, with K_i values of 1.6 μM and 51 nM at pH 7.5, respectively. We also demonstrate the inhibition of human type II arginase by the boronic acid-based transition-state analogues 2(*S*)-amino-6-boronohexanoic acid (ABH) and *S*-(2-boronoethyl)-L-cysteine (BEC), which are known inhibitors of type I arginase. At pH 7.5, both ABH and BEC are classical, competitive inhibitors of human type II arginase with K_i values of 0.25 and 0.31 μM, respectively. However, at pH 9.5, ABH and BEC are slow-binding inhibitors of the enzyme with K_i values of 8.5 and 30 nM, respectively. The findings presented here indicate that the design of arginine analogues with uncharged, tetrahedral functional groups will lead to the development of more potent inhibitors of arginases at physiological pH.

Arginases catalyze the divalent cation-dependent hydrolysis of L-arginine to yield L-ornithine and urea. Mammalian type I arginases (AIs[1]) are cytosolic and are found primarily in the liver where they function as the final enzyme of the urea cycle. In contrast, type II arginases (AIIs) are mitochondrial and extrahepatic in location and are believed to function in the net synthesis of ornithine for the production of polyamines, glutamate, and proline (*1*, *2*). Both arginase isoforms are believed to participate in the regulation of NO biosynthesis by competing with NOS for arginine and thereby downregulating NO production (*1*, *3*−*5*). Conversely, N^{ω}-hydroxy-L-arginine (NOHA), an intermediate in the reaction catalyzed by NOS, is a potent competitive inhibitor of type I arginase with a K_i value of 10−42 μM (*6*, *7*). In addition, inhibition of arginase activity by N^{ω}-hydroxy-*nor*-L-arginine (*nor*-NOHA), as well as other arginase inhibitors, in cells producing NO leads to an enhancement of NO production (*3*, *4*, *8*, *9*). These data indicate that arginases and NOSs are reciprocally regulated in vivo by localized NOHA and arginine concentrations (Scheme 1).

Human type II arginase (hAII) has been expressed in *E. coli* and purified to homogeneity (*10*). Human AII and the well-studied rat AI isozyme are ∼50% identical in amino acid sequence, both exist as trimers, and both require Mn^{2+} for catalytic activity. Additionally, metal ligands and key catalytic amino acid residues are conserved between the two isoforms. Despite the similarities between the arginase isozymes, isozyme-selective amino acid inhibitors have been identified (*10*). For example, L-ornithine, a product of the reaction catalyzed by arginase, is an inhibitor of the type I isozyme with a K_i value of 1 mM (*11*), while L-ornithine is a poor inhibitor of hAII with a K_i value greater than 10 mM (*10*). Such isozyme selectivity suggests that subtle differences exist within the active site structures of the two arginase isozymes. These differences have the potential to be exploited to develop more potent, isozyme-selective inhibitors of human type II arginase.

Due to the reciprocal regulation between arginases and NOS, the inhibition of arginase has recently become the focus of potential therapies for treating several NO-dependent smooth muscle disorders, including erectile dysfunction. Recent studies have shown that the addition of 2(*S*)-amino-6-boronohexanoic acid (ABH), a potent inhibitor of type I arginase (*3*, *4*, *12*), to rabbit penile corpus cavernosum and opossum internal anal sphincter muscles leads to an enhancement of NO-dependent smooth muscle relaxation (*3*, *4*). Also, the addition of *S*-(2-boronoethyl)-L-cysteine (BEC), another potent inhibitor of type I arginase, to human penile corpus cavernosum muscle results in the enhancement of NO-dependent smooth muscle relaxation (*8*). Since ABH and BEC are not inhibitors of NOS, it is likely that these synthetic boronic acid-based arginine analogues inhibit arginase in these muscles, leading to increased arginine concentrations for the biosynthesis of NO by NOS.

In this study, we have screened a series of arginine analogues as potential inhibitors of human type II arginase.

† This work was supported by NIH Grant DK44841.

* To whom correspondence should be addressed. Phone: (215) 707-4165. Fax: (215) 707-7536. E-mail: deash@astro.temple.edu.

[1] Abbreviations: NO, nitric oxide; NOS, nitric oxide synthase; AI, type I arginase; AII, type II arginase; hAII, human type II arginase; NOHA, N^{ω}-hydroxy-L-arginine; *nor*-NOHA, N^{ω}-hydroxy-*nor*-L-arginine; ABH, 2(*S*)-amino-6-boronohexanoic acid; BEC, *S*-(2-boronoethyl)-L-cysteine; TLC, thin-layer chromatography; HEPES, N-(2-hydroxyethyl)piperazine-*N*′-(2-ethanesulfonic acid); CHES, 2-(*N*-cyclohexylamino)ethanesulfonic acid; NMR, nuclear magnetic resonance.

10.1021/bi010783g CCC: $20.00
Published on Web 07/07/2001

Scheme 1

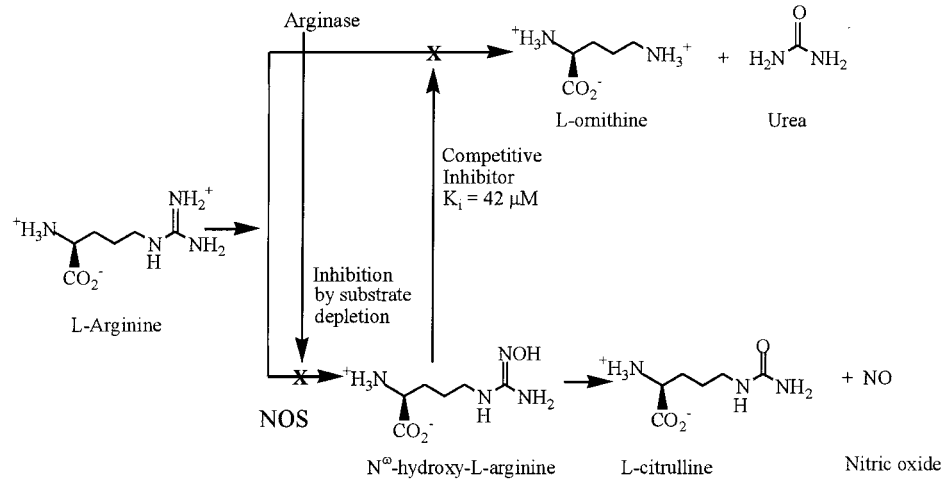

We report the potent inhibition of human AII by the classical inhibitors NOHA and *nor*-NOHA and the slow-binding inhibitors ABH and BEC. We also demonstrate the pH dependence of slow-binding inhibition by ABH and BEC.

EXPERIMENTAL PROCEDURES

Materials. Agmatine, L-canavanine, L-argininamide, L-argininic acid, L-homoarginine, and *E. coli* arginine decarboxylase were purchased from Sigma Chemical Co. ABH and BEC were provided by Dr. David W. Christianson, University of Pennsylvania. *nor*-NOHA was purchased from Bachem. All additional inhibitors were purchased from Alexis Biochemicals. L-[*guanido*-^{14}C]Arginine (specific activity 2.5 GBq mmol^{-1}) was purchased from NEN.

Purification. The mature form of human AII was expressed in *E. coli* BL21(DE3) and purified as described (*10*).

Synthesis of [guanido-^{14}C]Agmatine. [*guanido*-^{14}C]Agmatine was synthesized from L-[*guanido*-^{14}C]arginine following the procedure of Sastre et al. (*13*). A 50 μL sample of L-[*guanido*-^{14}C]arginine was added to a solution of 250 μL of 0.3 M sodium acetate, pH 5.2, that contained 10 units of *E. coli* arginine decarboxylase. Following incubation at 37 °C for 2 h, protein was precipitated by the addition of 0.5 mL of 100% ethanol and removed by centrifugation at 14 000 rpm for 10 min in a microfuge. The supernatant was dried under vacuum, dissolved in 90% ethanol, and stored as aliquots at −20 °C. The purity of the ^{14}C-labeled agmatine, evaluated by TLC, was estimated to be ≥90%.

Enzyme Assays with Agmatine and Classical Inhibitors. Assays of hAII activity utilizing agmatine as a substrate were performed at pH 7.5 as described (*10*) with [*guanido*-^{14}C]-agmatine replacing L-[*guanido*-^{14}C]arginine in the assay and with increasing concentrations of unlabeled agmatine. Evaluation of inhibitors was performed using the radioactive arginase assay as described (*10*) containing 100 μM $MnCl_2$ and either 100 mM HEPES−KOH, pH 7.5, or 100 mM CHES−KOH, pH 9.5. NOHA and *nor*-NOHA were evaluated as inhibitors of hAII at pH 7.5 by the addition of 2, 4, 6, and 10 μM NOHA or 0.05, 0.1, 0.2, and 0.3 μM *nor*-NOHA to the assay mixture. ABH and BEC were similarly evaluated as inhibitors of hAII at pH 7.5 by the addition of 0.1, 0.5, 1, and 2 μM ABH and 0.5, 1, 2, and 4 μM BEC to the assay mixture. Inhibition data were fit to the equation for competitive inhibition using the programs of Cleland (*14*). Inhibition constants for NOHA at pH 9.5 and for weak classical inhibitors (K_i > 5 mM) at pH 7.5 were determined by titrating a standard assay mixture containing 5 mM arginine with increasing concentrations of inhibitor. The K_i was estimated from the equation for competitive inhibition, although complete inhibition patterns were not determined for weak hAII inhibitors. Enzyme activity with L-argininamide, L-canavanine, L-homoarginine, and L-argininic acid as alternate substrates was measured with a coupled, spectrophotometric assay with urease and glutamate dehydrogenase (*11*).

Enzyme Assays with Slow-Binding Inhibitors. Slow onset inhibition of hAII by ABH and BEC at pH 9.5 was measured as described (*8*) by the addition of 0.14 μg of hAII to assay mixtures containing 100 mM CHES−KOH, pH 9.5, 100 μM $MnCl_2$, 10 mM unlabeled arginine, 0.05 μCi L-[*guanido*-^{14}C]arginine, and varying concentrations of ABH or BEC. Aliquots were removed at indicated times, and [^{14}C]urea was analyzed as described. Slow release kinetics were also analyzed as described (*8*) with the following modifications. The enzyme was incubated with 20 μM ABH or BEC for 15 min at room temperature and then diluted 100-fold into 1 mL of assay mixture, and the production of [^{14}C]urea was monitored as described. Inhibition constants were determined from the ratio of k_{off}/k_{on} and were also estimated from the final steady-state velocities using the equation for competitive inhibition. Complete release of ABH and BEC from hAII was examined by incubation of the enzyme in the presence of 30 μM of each inhibitor at room temperature for 30 min, followed by overnight dialysis against 50 mM CHES−KOH, pH 9.5. The samples were assayed for arginase activity the following day (∼16 h).

^{11}B NMR Studies. The p*K* of the boronic acid moiety of BEC was determined by monitoring the chemical shift change of the ^{11}B nucleus as a function of pH by NMR. ^{11}B (81.2% natural abundance, I = 3/2) NMR spectra were recorded on a Bruker Avance DRX 300 NMR spectrometer operating at 96.26 MHz. The following spectral parameters were employed: sweep width, 9615 Hz; pulse width, 90°; acquisition time, 0.85 s; line broadening, 10 Hz at a temperature of 295 K. Chemical shifts are referenced to external boron trifluoride diethyl etherate (Aldrich). Solutions

Table 1: Inhibitors of Human Type II Arginase. Guanido Compounds

Structure of Compound	Compound	Estimated K_i (mM)
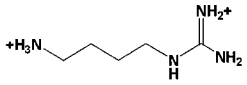	Agmatine	> 10
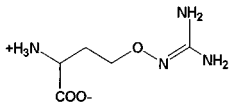	L-Canavanine	76
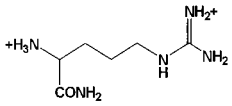	L-Argininamide	66
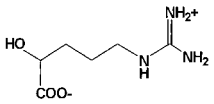	L-Argininic acid	271
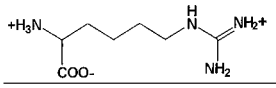	L-Homoarginine	39

contained 10 mM BEC, with 10% D_2O added for field-frequency lock. Chemical shift data were analyzed using eq 1, where δ is the chemical shift at a particular pH, δ_{acid} is the limiting chemical shift of the protonated, trigonal boronic acid, and δ_{base} is the limiting chemical shift of the unprotonated, tetrahedral boronate anion.

$$\delta = (\delta_{acid} + \delta_{base} \times 10^{pH-pK})/(1 + 10^{pH-pK}) \quad (1)$$

RESULTS

Classical Inhibitors of hAII. A variety of guanido compounds and arginine analogues were tested as inhibitors of hAII, and the kinetic constants are summarized in Tables 1 and 2, respectively. All of the guanido compounds and a majority of the arginine analogues analyzed were poor inhibitors of hAII, with the exception of N^{ω}-nitro-L-arginine, which has a K_i value of 6 mM, comparable to the K_M value of 5 mM arginine for hAII at pH 7.5. In addition, the guanido compounds shown in Table 1 were also tested as alternate substrates for hAII (data not shown). All of the compounds tested were at least 1000-fold less specific for hAII as compared to arginine, and no rate of hydrolysis could be detected for L-homoarginine, L-argininamide, or L-canavanine even at elevated enzyme concentrations. The best guanido compound utilized as a substrate for hAII at pH 7.5 is agmatine. The K_M of agmatine for hAII is estimated to be 12.5 mM, approximately 2.5-fold greater than the K_M of arginine for the enzyme. However, the k_{cat} for hAII utilizing agmatine as a substrate is 0.1 s^{-1}, compared to 203 s^{-1} with hAII utilizing arginine as a substrate.

Table 3 summarizes the kinetic constants for the potent inhibitors NOHA, *nor*-NOHA, ABH, and BEC. NOHA is a competitive inhibitor of hAII, as shown in Figure 1. The K_i of NOHA for hAII is 1.6 ± 0.1 μM at pH 7.5. At pH 9.5, the pH optimum of the enzyme, the K_i of NOHA for hAII is 2 μM, as estimated from initial velocity measurements. *nor*-NOHA is a potent competitive inhibitor of hAII, with a K_i value of 51 ± 8 nM at pH 7.5. Inhibition of hAII by *nor*-NOHA at pH 9.5 was not determined due to the instability of the compound at alkaline pH.

Table 2: Inhibitors of Type II Arginase. Arginine Analogues

Structure of Compound	Compound	Estimated K_i (mM)
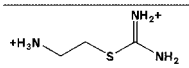	S-(2-Aminoethyl)isothiourea	25
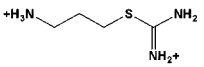	S-(3-Aminopropyl)isothiourea	16
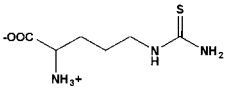	L-Thiocitrulline	9
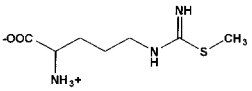	S-Methyl-L-thiocitrulline	15
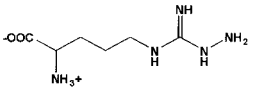	N^{ω}-Amino-L-arginine	20
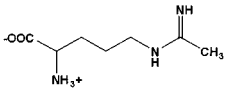	L-N^5-(1-Iminoethyl)-ornithine	42
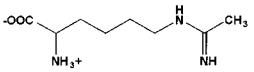	L-N^6-(1-Iminoethyl)-lysine	77
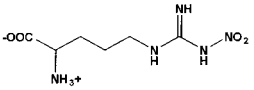	N^{ω}-Nitro-L-arginine	6

Table 3: Potent Competitive Inhibitors of Type II Arginase

Inhibitor	K_i	Type of Inhibition
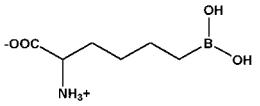 ABH	K_i at pH 9.5 = 8.5 nM	slow binding
	K_i at pH 7.5 = 0.25 μM	competitive
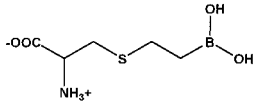 BEC	K_i at pH 9.5 = 30 nM	slow binding
	K_i at pH 7.5 = 0.31 μM	competitive
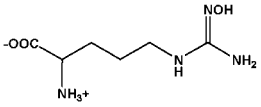 NOHA	K_i at pH 9.5 = 2 μM	competitive
	K_i at pH 7.5 = 1.6 μM	competitive
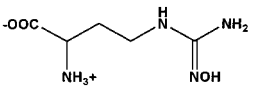 *nor*-NOHA	K_i at pH 7.5 = 51 nM	competitive

Slow-Binding Inhibitors of hAII. At pH 7.5, ABH and BEC are potent classical inhibitors of hAII with K_i values of 0.25 ± 0.05 and 0.31 ± 0.04 μM, respectively. However, at pH 9.5 the progress curves for arginine hydrolysis in the presence of ABH and BEC are nonlinear, as shown in Figures 2 and 3, respectively. The nonlinearity of the progress curves is indicative of slow-binding inhibition, typically characterized

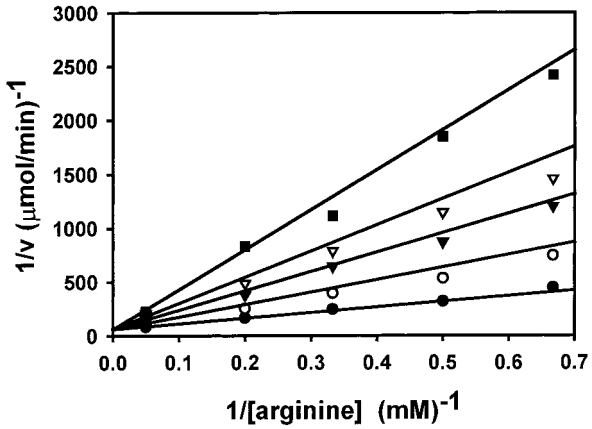

FIGURE 1: Inhibition of hAII by NOHA. NOHA concentrations were 0 (closed circles), 2 (open circles), 4 (closed triangles), 6 (open triangles), and 10 μM (closed squares), and assays were conducted at pH 7.5 as described in the Materials and Methods. The solid lines are the fits of the data to the equation for competitive inhibition.

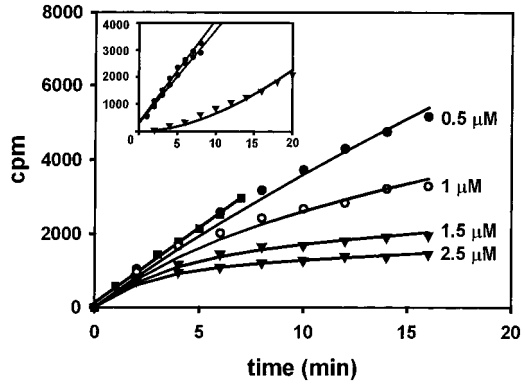

FIGURE 2: Slow-binding inhibition of hAII by ABH at pH 9.5. Progress curves were generated as described in the Materials and Methods at the indicated concentrations of ABH. The curves represent the best fits of the data to eq 2. Inset: release of ABH from the arginase−ABH complex. The straight lines correspond to a control assay performed in the absence of ABH and an assay carried out in the presence of 0.2 μM ABH. The curve represents the regain of activity following a 100-fold dilution of the preformed arginase−ABH complex to give a final concentration of 0.2 μM ABH. The lines represent the best fits of the data to eq 2.

by the rapid formation of a reversible E•I complex followed by a slow isomerization or conformational change to yield the inhibitory E•I* complex (Scheme 2).

Progress curves for the arginase-catalyzed production of urea in the presence of ABH and BEC at pH 9.5 were fit by nonlinear least-squares analysis to the integrated expression

$$P = v_s(t) + (v_o - v_s)(1 - e^{-k_{obs}(t)})/k_{obs} \quad (2)$$

where P is the amount of urea formed (cpm), v_o is the initial rate of urea formation, v_s is the steady-state rate of urea formation, and k_{obs} is the apparent first-order rate constant for the establishment of the equilibrium between E•I and E•I* (*15*). Within the limitations of the assay, the initial velocities (v_o) appear to be independent of inhibitor concentration, suggesting that the dissociation constant for the E•I complex must be larger than the range of inhibitor concentrations used to generate the progress curves. Due to these limitations, the steady-state intermediate E•I is not observed,

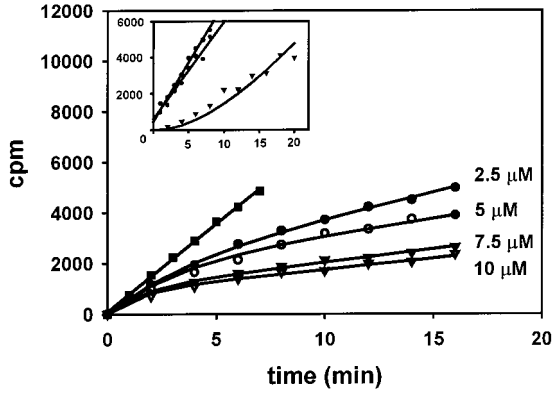

FIGURE 3: Slow-binding inhibition of hAII by BEC at pH 9.5. Progress curves were generated as described in the Materials and Methods at the indicated concentrations of BEC. The curves represent the best fits of the data to eq 2. Inset: release of BEC from the arginase−BEC complex. The straight lines correspond to a control assay performed in the absence of BEC and an assay carried out in the presence of 0.2 μM BEC. The curve represents the regain of activity following a 100-fold dilution of the preformed arginase−BEC complex to give a final concentration of 0.2 μM BEC. The lines represent the best fits of the data to eq 2.

Scheme 2

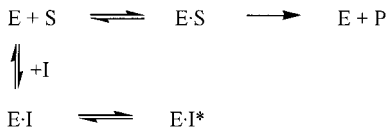

Scheme 3

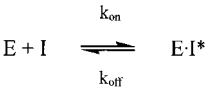

and therefore the binding of inhibitor to hAII is approximated as a single-step process with $K_i = k_{off}/k_{on}$ (Scheme 3).

The association rate constant k_{on} was estimated from a plot of k_{obs}, determined from an analysis of the progress curves using eq 2, versus inhibitor concentration according to eq 3.

$$k_{obs} = k_{off} + k_{on}[I]/(1 + [S]/K_M) \quad (3)$$

The dissociation rate constant, k_{off}, was determined by monitoring the rate of the return of activity from the enzyme−inhibitor complex via eq 2. Replots of k_{obs} versus [ABH] yield $k_{on} = 8.4 \times 10^4$ M^{-1} s^{-1}, and those of k_{obs} versus [BEC] yield $k_{on} = 3.65 \times 10^4$ M^{-1} s^{-1}. The best fits of inhibitor release data (Figures 2 and 3, inset) yield $k_{off} = 7.1 \times 10^{-4}$ s^{-1} for ABH and $k_{off} = 1.11 \times 10^{-3}$ s^{-1} for BEC. The resultant K_i values of 8.5 nM for ABH and 30 nM for BEC calculated from these rate constants are in good agreement with the values of 4.6 and 49 nM for ABH and BEC, respectively, estimated from the steady-state velocities (data not shown).

To test for the reversibility of inhibition, samples of hAII were incubated with 30 μM ABH or BEC at pH 9.5 for 30 min. The samples were then dialyzed overnight versus 50 mM CHES−KOH, pH 9.5, and assayed for enzymatic activity. Both enzyme samples regained full activity as compared to an untreated sample of the enzyme. Thus, inhibition of hAII by ABH and BEC is fully reversible.

^{11}B NMR Characterization of BEC. The ^{11}B NMR spectrum of BEC exhibits a broad resonance (line width of 260

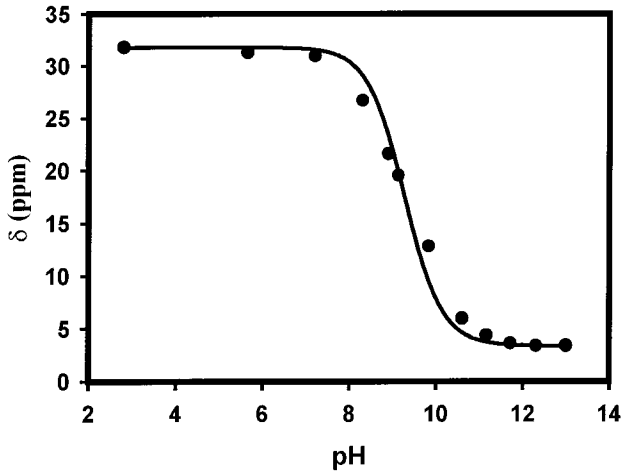

FIGURE 4: ^{11}B NMR chemical shifts of BEC as a function of pH. The solid line is a fit of the data to eq 1.

Hz) 31.8 ppm downfield of boron trifluoride diethyl etherate at pH 2.8. Titration of this sample with KOH results in an upfield shift of this resonance, as seen in Figure 4, that is accompanied by a sharpening of the ^{11}B resonance (line width of 120 Hz) as the trigonal boronic acid is converted to the tetrahedral boronate. Fits of the chemical shift data as a function of pH according to eq 1 yield a p*K* of 9.3 ± 0.1 for the boronic acid moiety of BEC.

DISCUSSION

Since arginase and NOS utilize arginine as a common substrate, arginase competes with NOS for arginine, thus downregulating the biosynthesis of NO, a potent molecule involved in neurotransmission, innate immunity, and vascular regulation. Recent studies have shown that type I and type II arginases are located extrahepatically (for a review see ref *16*), and therefore both isozymes may be involved in the regulation of NO production in mammals. For example, type II arginase is induced early in lipopolysaccharide-stimulated mouse macrophages, while the type I isozyme is induced much later. It is believed that elevated type II arginase activity is involved in producing ornithine for the biosynthesis of proline and polyamines, necessary for wound healing, while elevated type I arginase activity prevents the overproduction of toxic NO. The inhibition of arginases may therefore upregulate NO biosynthesis by increasing the availability of arginine for NOS. These studies imply that arginase is a therapeutic target for the treatment of diseases of impaired NO production, such as erectile dysfunction. In addition, with the availability of purified hAII, the kinetic and structural differences between the arginase isozymes are becoming apparent and may therefore be exploited therapeutically.

The guanido compounds shown in Table 1 are extremely poor inhibitors of and substrates for hAII. In comparison, these compounds are respectable substrates for rat liver arginase, with k_{cat}/K_M values ranging between 10^2- and 10^5-fold less than the k_{cat}/K_M for rat AI utilizing arginine as a substrate (*11*). Although agmatine is the poorest alternate substrate for rat AI, it is the best alternate substrate for hAII. However, agmatine is 1000-fold less specific as a substrate for hAII as compared to arginine. While the k_{cat}/K_M of hAII utilizing arginine as a substrate is 6.33×10^4 M^{-1} s^{-1}, the k_{cat}/K_M value for agmatine as a substrate is 1.02×10^1 M^{-1} s^{-1}. It is interesting to note that agmatine is a very poor substrate for hAII. Recent evidence has suggested that agmatine may be a novel neurotransmitter in mammalian systems (*17*), and agmatinase activity, catalyzing the hydrolysis of agmatine to yield putrescine and urea, has recently been localized to the mitochondrial matrix of several mammalian cell lines (*13*, *18*). However, no mammalian agmatinase has been cloned or purified thus far. On the basis of the current data, it is unlikely that agmatine is a physiologic substrate for type II arginase. Additionally, the arginine analogues listed in Table 2 are also poor inhibitors of hAII, while many of these compounds are known inhibitors of NOS isoforms (*19*). Collectively, these data demonstrate the strict requirements for the constituents about C-α, the chain length, and the p*K* of the guanidinium group of substrates and/or inhibitors of hAII. Furthermore, with the exception of the N^{ω}-hydroxy substitution (e.g., NOHA), substitutions at the N^{ω}-positions are poorly tolerated by hAII, while many of these compounds are potent inhibitors of NOS isoforms.

Arginases regulate the biosynthesis of NO by depleting arginine, the substrate of NOS, while NOS regulates the activity of both arginase isozymes due to the inhibition of arginases by NOHA, the stable intermediate of the reaction catalyzed by NOS (*1*, *3*−*5*). While NOHA is a potent inhibitor of rat liver arginase with a K_i value of 10−42 μM (*6*, *7*), the data presented herein reveal that the inhibition of hAII by NOHA, with a K_i value of 1.6 μM, is approximately 20-fold tighter than the inhibition of rat AI. *nor*-NOHA is the best inhibitor of hAII identified at physiological pH, with a K_i value of 51 nM. While *nor*-NOHA is a potent competitive inhibitor of rat liver arginase with a K_i value of 0.5 μM (*6*), *nor*-NOHA is ∼10-fold more potent as an inhibitor of hAII as compared to the type I isozyme. Collectively, the inhibition data show that *nor*-NOHA is ∼40-fold more potent than NOHA for the inhibition of hAII, while both NOHA and *nor*-NOHA are more potent inhibitors of hAII as compared to the type I isozyme.

ABH and BEC are known slow-binding inhibitors of type I arginase (*3*, *8*), and the equilibrium ionization of these boronic acids is shown in Figure 5A. Although the p*K* values for boronic acids are often estimated on the basis of the p*K* for methane boronic acid (p*K* of 11.2−11.4), recent data have indicated that this approximation may not be valid for amino acid analogues containing a boronic acid moiety (*20*). For example, the p*K* of the boronic acid moiety of L-2-amino-4-boronobutanoic acid is 7.9, and it has been suggested that this lower p*K* results from a conformation that places the boronic acid moiety close to the α-amino group. Consistent with this hypothesis, the ^{11}B NMR titration data for L-2-amino-4-boronobutanoic acid show a second p*K* that has been attributed to titration of the α-amino group (*20*). The p*K* for the boronic acid of BEC is 9.3, and the NMR data show no evidence for a similar interaction between the boronic acid moiety and the α-amino group. Such an interaction would require the formation of a seven- to eight-membered ring system, which is likely to be less favorable than the five- to six-membered ring system formed in the case of L-2-amino-4-borono-butanoic acid.

Crystal structures of rat AI complexed with ABH and BEC (*4*, *8*) reveal that the tetrahedral species of the boronic acids

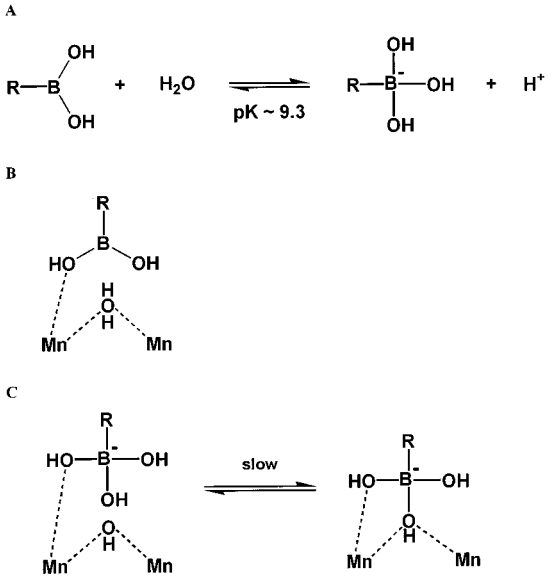

FIGURE 5: (A) Ionization equilibrium between the trigonal and tetrahedral species of the boronic acid inhibitors of hAII. (B) Proposed mechanism for inhibition of arginases by ABH and BEC at pH 7.5. (C) Proposed mechanism for inhibition of arginases by ABH and BEC at pH 9.5. For ABH, R = $(NH_3^+)(COO^-)CH(CH_2)_{4-}$. For BEC, R = $(NH_3^+)(COO^-)CHS(CH_2)_{2-}$.

are bound in the active site of the enzyme at alkaline pH. Addition of ABH and BEC to corpus cavernosum smooth muscles results in an increase in NO-dependent smooth muscle relaxation. This enhanced smooth muscle relaxation presumably results from the inhibition of arginase by these compounds, thus increasing the arginine pool for NOS. The data presented here reveal for the first time the direct inhibition of hAII by ABH and BEC. ABH is the most potent inhibitor of hAII reported thus far, with a K_i value of 8.5 nM at pH 9.5, the pH optimum of hAII, as compared to the K_M of arginine for hAII, which is 0.3 mM at pH 9.5.

Both ABH and BEC could bind to arginase by one or two routes, either the binding of the trigonal species and subsequent attack by the nucleophilic solvent molecule to yield the tetrahedral boronate species, which has been postulated by Kim et al. (*8*), or direct binding of the tetrahedral species to the active site of the enzyme. The former implies that the activated metal-bridging solvent molecule must attack the boronic acid inhibitor, resulting in the formation of the tetrahedral species that mimics the proposed tetrahedral intermediate of the reaction catalyzed by arginases (*21*). The latter route suggests that the tetrahedral boronate species may bind to the enzyme directly and displace the metal-bridging solvent molecule.

At pH 7.5, ABH and BEC are potent inhibitors of hAII, but they are not slow-binding inhibitors. Slow-binding inhibition of hAII by the boronic acids is observed at a pH ≥ 9.0, while these compounds demonstrate classical inhibition of hAII at pH 8.5 (data not shown). The classical inhibition by ABH and BEC at pH 7.5 likely results from the binding of the trigonal species of each compound, which predominates over the tetrahedral species by about 60-fold at this pH, to the active site of hAII. However, at pH 9.5, the tetrahedral species predominates by 1.6-fold over the trigonal species of the boronic acids. The pH dependence of slow-binding inhibition by ABH and BEC suggests that the tetrahedral species of each inhibitor is the slow-binding species for inhibition of hAII. Since the active site of an enzyme is designed to bind its substrate but not designed to directly bind the transition-state molecule, an enzyme would probably need to undergo an active site conformational change to bind a transition-state analogue efficiently (*15*). This structural readjustment may therefore cause the slow step of inhibition by a slow-binding, transition-state analogue, such as ABH and BEC. In addition, the pH dependence of the catalytic activity of hAII reveals that one group on the enzyme, believed to be the metal-bound solvent molecule, must be deprotonated for optimal activity, with a p*K* of 9.3 in the free enzyme that decreases to a p*K* of 7.9 upon substrate binding (*10*). Given these data, we propose that the binding of the trigonal species of ABH and BEC results in the classical inhibition of hAII by these compounds at pH 7.5, as shown in Figure 5B. At pH 7.5, it is likely that the solvent-derived metal-bridging ligand is a water molecule and not an activated hydroxide ion. This metal-bridging water molecule would be unlikely to attack the trigonal species of the boronic acid inhibitors to produce the tetrahedral boronate. Furthermore, analysis of the crystal structure for the native rat AI indicates that an open coordination site exists on Mn_A (*21*). Only partial occupancy of this site by solvent water is observed in the crystal structure, and it is proposed that this site provides the initial interaction between the boronic acids and the metal center of both arginase isoforms. Additionally, it is proposed that the fast step of inhibition of hAII by ABH and BEC at pH 9.5 occurs as the tetrahedral boronic acid binds to hAII directly, followed by the slow step, in which the metal-bound hydroxide molecule must be displaced by a hydroxyl group of the boronic acid, as shown in Figure 5C. Studies are currently being performed to obtain a crystal structure of rat AI with ABH and BEC bound at neutral pH. The findings presented here indicate that arginine analogues with uncharged, tetrahedral functional groups may be more potent, slow-binding inhibitors of arginases at physiological pH.

ACKNOWLEDGMENT

We thank Dr. S. M. Morris, Jr., for helpful suggestions. We also thank Dr. G. D. Markham for assistance in collecting the NMR data.

REFERENCES

1. Li, H., Meininger, C. J., Hawker, Jr., J. R., Haynes, T. E., Kepka-Lenhart, D., Mistry, S. K., Morris, Jr., S. M., and Wu, G. (2001) *Am. J. Physiol. Endocrinol. Metab. 280*, E75−E82.
2. Wu, G., and Morris, Jr., S. M. (1998) *Biochem. J. 336*, 1−17.
3. Baggio, R., Emig, F. A., Christianson, D. W., Ash, D. E., Chakdar, S., and Rattan, S. (1999) *J. Pharmacol. Exp. Therapeut. 290*, 1409−1416.
4. Cox, J. D., Kim, N. N., Traish, A. M., and Christianson, D. W. (1999) *Nat. Struct. Biol. 6*, 1043−1047.
5. Gotoh, T., and Mori, M. (1999) *J. Cell Biol. 144*, 427−434.
6. Custot, J., Moali, C., Brollo, M., Boucher, J. L., Delaforge, M., Mansuy, D., Tenu, J. P., and Zimmermann, J. L. (1997) *J. Am. Chem. Soc. 119*, 4086−4087.
7. Daghigh, F., Fukuto, J. M., and Ash, D. E. (1994) *Biochem. Biophys. Res. Commun. 202*, 174−180.
8. Kim, N. N., Cox, J. D., Baggio, R. F., Emig, F. A., Mistry, S. K., Harper, S. L., Speicher, D. W., Morris, Jr., S. M., Ash, D. E., Traish, A., and Christianson, D. W. (2001) *Biochemistry 40*, 2678−2688.

9. Tenu, J. P., Lepoivre, M., Moali, C., Brollo, M., Mansuy, D., and Boucher, J. L. (1999) *Nitric Oxide 3*, 427−438.
10. Colleluori, D. M., Morris, Jr., S. M., and Ash, D. E. (2001) *Arch. Biochem. Biophys. 389*, 135−143.
11. Reczkowski, R. S., and Ash, D. E. (1994) *Arch. Biochem. Biophys. 312*, 31−37.
12. Baggio, R., Elbaum, D., Kanyo, Z. F., Carroll, P. J., Cavalli, R., Ash, D. E., and Christianson, D. W. (1997) *J. Am. Chem. Soc. 119*, 8107−8108.
13. Sastre, M., Regunathan, S., Galea, E., and Reis, D. J. (1996) *J. Neurochem. 67*, 1761−1765.
14. Cleland, W. W. (1979) *Methods Enzymol. 63*, 103−138.
15. Morrison, J. F., and Walsh, C. T. (1988) *Adv. Enzymol. 61*, 201−301.
16. Mori, M., and Gotoh, T. (2000) *Biochem. Biophys. Res. Commun. 275*, 715−719.
17. Reis, D. J., and Regunathan, S. (1998) *J. Auton. Nerv. Syst. 72*, 80−85.
18. Sastre, M., Galea, E., Feinstein, D., Reis, D. J., and Regunathan, S. (1998) *Biochem. J. 330*, 1405−1409.
19. Stuehr, D. J., and Griffith, O. W. (1992) *Adv. Enzymol. 65*, 287−347.
20. London, R. E., and Gabel, S. A. (2001) *Arch. Biochem. Biophys. 385*, 250−258.
21. Kanyo, Z. F., Scolnick, L. R., Ash, D. E., and Christianson, D. W. (1996) *Nature 383*, 554−557.

BI010783G